Redox-dependent Structural Origin of the Temperature Threshold and Sensitivity in the TRPV3 Bio-thermometer

Guangyu Wang (gary.wang10@gmail.com)
University of California Davis https://orcid.org/0000-0002-5581-6926

Research Article

Keywords: gating loop, graph theory, hairpin thermodynamics, ion channel, non-covalent interaction, redox-dependence, thermo-sensitivity, threshold, use-dependent sensitization

Posted Date: June 16th, 2022

DOI: https://doi.org/10.21203/rs.3.rs-1556082/v9

Redox-dependent Structural Origin of the Temperature Threshold and Sensitivity in the TRPV3 Bio-thermometer

Guangyu Wang*

Department of Physiology and Membrane Biology, University of California School of Medicine, Davis, CA, USA

Department of Drug Research and Development, Institute of Biophysical Medico-chemistry, Reno, NV, USA

* Author to whom correspondence should be addressed; E-mail: gary.wang10@gmail.com

Abstract

The DNA hairpin with a limited size is sensitive to temperature. However, it is unclear if thermosensitive TRP channels also use the temperature-dependent little hairpin sizes to govern their temperature thresholds and sensitivity. Here, graph theory was used as a novel tool to test this hypothesis by analyzing the redox- and state-dependent cryo-electron microscopy structures of TRPV3 with or without the Y564A mutation at different temperatures. The results showed that the biggest little hairpin with the minimum topological loop size and strength control the temperature threshold while a change in the total minimum little hairpin sizes upon a change in the total non-covalent interactions along the channel gating pathway governs the temperature sensitivity. This size- and strength-dependent hairpin thermodynamics may tune the thermal activity and sensitivity of biological macromolecules. (129 words)

Keywords: gating loop; graph theory; hairpin thermodynamics; non-covalent interaction; redox-dependence; thermo-sensitivity; threshold; TRP channel; use-dependent sensitization

1. INTRODUCTION

The transient receptor potential (TRP) channels can be gated by both physical and chemical stimuli to conduct cations. Among 28 mammalian members in the TRP superfamily, eleven ones are thermosensitive through a variety of TRP channel families including TRPV (vanilloid), TRPM (melastatin), TRPC (canonical), and TRPA (ankyrin). Their temperature thresholds (T_{th}) for activation range from noxious cold, cold, warm to noxious heat. Specifically, TRPV1 (>42°C), TRPV2 (>52°C), TRPV3 (>32–39°C), TRPV4 (>25–35°C), TRPM2, TRPM3, TRPM4, and TRPM5 are involved in warm to hot sensation. In contrast, TRPA1 (<17°C) or TRPM8 (<20–28°C) and TRPC5 (<25-37°C) are sensitive to cold and cool temperatures. These thermosensitive TRP channels also have a high temperature sensitivity Q_{10} compared to non-temperature-sensitive ones [1-16]. However, the origin of their temperature threshold and sensitivity is unknown.

A critical clue comes from a DNA hairpin thermal biosensor. Its hairpin sizes within 20 bases in the loops can produce temperature thresholds in a range of those thermosensitive TRP channels. The larger hairpin size and the less H-bonds in the stem generally have the lower threshold. Its initial melting curve also has a characteristic slope as the temperature sensitivity (Q_{10}=1.8-2.7) [17]. Therefore, it is exciting to ask if the temperature-dependent biggest little hairpin with the minimum loop size and strength along the gating pathway of thermosensitive TRP channels initiates an activation threshold while a change in the total minimum little hairpin sizes between closed and open states of a single channel upon a change in the total non-covalent interactions controls Q_{10}. The recent state- and redox-dependent cryo-electron microscopy (cryo-EM) structures of mTRPV3 with or without the Y564A mutation at different temperatures may provide an opportunity for graph theory to be used as a novel tool to examine the hypothesis [18-20]. In addition, mTRPV3 undergoes sensitization while TRPV1, 2 and 4 channels desensitize upon successive heat stimuli [7, 18-24]. Thus, the role of the redox state of mTRPV3 in use-dependent sensitization was also investigated. Once such a hairpin thermodynamic model was applied to this thermo-gated cation channel, the calculated melting temperatures (T_m) and structural thermo-sensitivity (Ω_{10}) values were commensurable to the experimental thresholds (T_{th}) and functional thermo-sensitivity (Q_{10}) values, respectively. In this regard, TRPV3 may use a change of temperature-dependent biggest little hairpin size and strength to detect different temperatures with a high sensitivity.

2. RESULTS

2.1. The Definition of the Least Gating Pathway of mTRPV3

mTRPV3 is mainly expressed in skin keratinocytes and oral and nasal epithelia, mediating thermal reception and pain sensation [5-6]. Like other TRPV channels, TRPV3 is a homotetramer. Each monomer has S1-S6 as a transmembrane domain (TMD) and a large intracellular amino- (N-) terminal as an ankyrin repeat domain (ARD). S1-S4 form a voltage-sensor-like domain (VSLD) while S5-S6 and the pore helix and two pore loops are folded as a pore domain. Both the VSLD and the pore domain are swapped via a S4−S5 linker. The TRP helices, which are almost parallel to the membrane, interact with both the skirt ARD and the TMD. Several lipid sites were also found in their interfaces. The pre-S1 domain, together with the carboxy- (C-) terminal loop domain, couples the TMD with the ARD. The residues ^{638}GLGD^{641} in the P-loop-extended region line the selectivity filter to permeate partially hydrated Na^+ , K^+ or Ca^{2+} ions but not to function as an upper gate. In contrast, the narrowest pore constriction around M677 on S6 may act as a lower gate Since the interaction of the pre-S1 domain with the TRP domain constitutes a sealed large loop so that the heat-evoked conformational change can be extended in the loop, the least gating pathway of mTRPV3 should include at least the pre-S1 domain and the TRP domain. [18, 21]

2.2. The First Biggest Little Hairpin in the VSLD/pre-S Interface Set a Temperature Threshold 42°C for Oxidized mTRPV3

C612 and C619 in the outer pore of mTRPV3 can form a disulfide bond upon oxidization [18]. In the closed state at 42°C, the diversity of non-covalent interactions between amino acid side chains in oxidized mTRPV3 could produce multiple little hairpins along the gating pathway from D396 in the pre-S1 domain to K505 in the TRP domain.

First, H-bonds emerged between different hydrophilic residues. In the pre-S1/TRP interface, the H-bonding pairs T397-K432/E704 sealed the largest hairpin loop from T397 to E704. In the VSLD, the H-bonding pairs included Y448/Y451-Q529, T456-W559, K500-E501, D512-Q514/S515, Y564-R567. In the VSLD/S4-S5 linker/TRP interfaces several H-bonding pairs were found such as T566-S576, R567-T699, Q570/R693-E689 and R698-E702. In the pore domain, H-bonds were formed among pairs including D586-T680, Y594-Y661/T636-Y661, E610/K614-N647, S621-Q646, S624-D627, E631-K634 and E682-K686. In addition, the vanilloid site phosphatidylcholine (PC) also related W521 on S3 to Q695 in the TRP domain via two H-bonds (Fig. 1A-B).

Second, several aromatic residues were involved in π interactions with nearby residues. For example, W433/W692-R696/K438 in the TRP/pre-S1 interface; F441-W433/Y565 in the pre-S1/VSLD interface; F445-F449/Y565, F447/Y451-W493, Y448-F526/Y565, F449-W559, H471-Y540/Y547, F489-W493, W521-F522/F524, F522/Y564-F526, F524-V528, F527-V531, Y540-Y547, F542-Y544, and Y564-Y565 in the VSLD; Q570-W692 and Y575-I579 in the S4-S5 linker/TRP interface; F590-Y594/L673, F597-F601/L664, F601/T665-Y661, Y622/Q646-F654, F625-V629 and F656-T660 in the pore domain (Fig. 1A).

Third, salt bridges were also present between several charged pairs. They covered D396/E704-K432 in the TRP/pre-S1 interface, R416-D519 in the VSLD/pre S1 interface, E610-K614 in the outer pore, and E687-R690 in the TRP domain (Fig. 1A).

Taken together, despite several smallest little hairpins with no residue in the loops, the first biggest little hairpin with a minimum 17-residue loop appeared in the VSLD/pre-S1 interface to control the D519-R416 salt bridge (Fig. 1C-D). It started with D519 and went through W521, F522, Y564, Y565, F441, W433 and ended with R416 (Fig. 1E). Based on two equivalent H-bonds in the loop, the predicted melting temperature was about 40°C (Table 1), which was close to the threshold 42°C for the activation of oxidized mTRPV3. [18] The total numbers of all non-covalent interactions and little hairpin sizes with minimum loops along the gating pathway from D396 to K705 were 69 and 99, respectively (Fig. 1A).

2.3. Oxidized mTRPV3 Opened at 42°C with Melting of the 1st Biggest Little Hairpin

In the heat-activated open state, when the disruption of the R416-D519 salt bridge melted the first biggest little hairpin at 42°C as predicted (Table 1), several changes were observed with the release of the PC lipid from the nearby W521 in oxidized mTRPV3.

First, in the VSLD/pre-S1 interface, the D519-R416 salt bridge was substituted by the N410-R509 and S515-T411-R416 H-bonds. As a result, the T397-K432 H-bond was broken with the formation of S402-E405 and E418-R690 and E423-T427 H-bonds in the TRP/pre-S1 interface. On the other hand, the H-bonds shifted from D512-Q514/S515 to D512-S518 in the VSLD (Fig.2A).

Second, when R567 formed a stimulatory H-bond with D519 in the VSLD, a little hairpin with a minimum 1-residue loop appeared from D519 to W521, F522, Y564, R567 and back to D519. As a result, the W521/V528-F524 and F522-F526 π interactions were disconnected with the change of the Y564-R567 H-bond to a cation-π interaction (Fig. 2A).

Table 1 The hairpin thermodynamic model-based new parameters of the mTRPV3 bio-thermometer along the gating pathway from D396 to K705

Constructs	**mTRPV3**			**mTRPV3-Y564A**	
PDB ID	6LGP	7MIO	7MIN	6PVP	6PVO
Lipid PC	bound	free	bound	free	free
Redox state	reduced	oxidized	oxidized	reduced	reduced
Lipid environment	MSP2N2	cNW11	cNW11	detergent	
Sampling temperature	**4°C**	**42°C**	**42°C**	**37°C**	**37°C**
Gating state	closed	open	closed	open	closed
# of the biggest little hairpin	3	2	1	5	4
Biggest little loop size (L_{max}), a.a	12	9	17	14	13
Equivalent H-bonds in L_{max}	2.0	2.0	2.0	3	1.0
Total non-covalent interactions	69	59	69	45	44
Total little hairpin sizes, a.a.	101	72	99	90	92
Calculated T_m	**50°C**	56°C	**40°C**	56°C	**38°C**
Measured threshold (T_{th})	**50°C**		**42°C**		**37°C**
Calculated $\Omega_{10,\ min}$	10.2		9.34		0.51
Calculated $\Omega_{10,\ mean}$	**22.8**		**21.0**		**1.00**
Calculated $\Omega_{10,\ max}$	82.6		76.0		2.93
Measured $Q_{10,}$	**21.2-27**		**27.0**		**1.21**
Ref. for measured T_{th} & Q_{10}	[19, 25, 26]		[18]		[19]

Note: $\Omega_{10,\ min,\ mean,\ max}$ were calculated when E=0.5, 1, 3 kJ/mol for the minimum, mean and maximal intensity of a non-covalent interaction in a minimum hairpin topological loop, respectively.

Third, when the conformational wave extended to the VSLD/S4-S5/TRP interfaces, the Q570-E689 H-bond and Y575-I579 π interaction and the E687-R690 salt bridge were disrupted. In the meantime, the H-bond shifted from R567-T699 to R567-Q695 (Fig. 2A).

Fourth, when this conformational wave continued to the pore domain, those F597-F601/L664 π interactions and E610-K614 salt bridge and N647-E610/K614 H-bonds were disconnected. In the meanwhile, F633 formed a CH-π interaction with I637, and the H-bond moved from S621-Q646 to S620-Q646 pairs (Fig. 2A).

Taking together, after the first biggest little hairpin with a minimum 17-residue loop in the VSLD/pre-S1 interface melted above the predicted 40°C, the biggest little hairpin moved to the S5-S6 interface (Fig. 2B). It had two equivalent H-bonds in a minimum 9-residue loop from D586 to F590 and L673 and T680 and back to D586 (Figs. 2C, E). Its melting temperature was about 56°C (Table 1). In the meanwhile, a little hairpin with a minimum 3-residue loop in the pre-S1/VSLD/S4-S5 linker/TRP/pre-S1 interfaces may be required to stimulate the lower state of the channel. It linked about 17 residues together, including T411, R416, H417, E418, R690, E689, R693, W692, R696, Q695, R567, D519, S518, D512 and S515 (Figs. 2D, E). As a result, the total numbers of all non-covalent interactions and minimum little hairpin sizes along the gating pathway from D396 to K705 dramatically decreased from 69 and 99 to 59 and 72, respectively (Fig. 2A). Such a major decrease was enough to produce a high structural thermo-sensitivity Ω_{10} in a range from 9.34 to 76.0 and with a mean value 21.0, which was comparable to the experimental functional thermo-sensitivity Q_{10} (~27) (Table 1). [18]

2.4. Binding of the PC Lipid to the Vanilloid Site Induced the Third Biggest Little Hairpin for the High Threshold of Reduced mTRPV3

In the closed state without the C612-C619 disulfide bond, reduced mTRPV3 at 4°C was different than oxidized one. In the pore domain, when the E610-K614 salt bridge and the E610-N647 and S621-Q646 H-bonds were disrupted, the E610-T649 and K614-S620 H-bonds and the F633-I637 π interaction emerged (Fig. 3A).

When this conformational change extended to the S4-S5 linker/TRP/S6 interfaces, the E682-K686 and R698-E702 H-bonds and the E687-R690 salt bridge were broken with the shift of the H-bond from R567-T699 to R567-Q695 (Fig.3A). As a result, in the TRP/pre-S1 interface, the R698-E702 H-bond was disrupted while the Y409-K705 and H417/E418-R690 H-bonds were created. In the VSLD/pre S1 interface, D519 formed an additional H-bond with T411. In the VSLD, the H471-Y540/Y547 π interactions were disconnected with the π interaction moving from F542-Y544 to Y540-Y544 and the H-bond shifting from D512-Q514 to Q514-S518. When the PC bridge moved from W521-PC-Q695 to W521-PC-F524/R567, H523 formed a π interaction with E501 and the Y564-R567 H-bond became a cation-π interaction. More importantly, in addition to a salt bridge between R567 and the PC lipid, the CH-π interactions of the PC lipid with W521 and F524 produced the third biggest little hairpin with two equivalent H-bonds in a minimum 12-carbon loop (Fig. 3B-D). The predicted melting temperature was about 50°C (Table

1), in agreement with the initial experimental threshold 50°C for TRPV3 opening. [26] On the other hand, reduced mTRPV3's total numbers of all non-covalent interactions and minimum hairpin sizes along the gating pathway from D396 to K705 were 69 and 101, respectively (Fig. 3A). When the same open state was employed (Fig.2A), the calculated structural thermo-sensitivity Ω_{10} was in a range from 10.2 to 82.6 and with a mean value 22.8, which was comparable to the experimental functional thermo-sensitivity Q_{10} (21.7-27) (Table 1). [19, 26]

2.5. Release of the PC Lipid from the Vanilloid Site by the Y564A Mutation Decreased the Temperature Threshold of Reduced mTRPV3

When reduced mTRPV3 had a mutation Y564A on S4, the disruption of the Y564-F522/F526/Y565/R567 π interactions not only released the PC lipid from the vanilloid site but also induced several changes along the gating pathway from D396 to K705 (Fig. 4A)[19]. In the VSLD, when the F522-F526 and Y540-Y544/Y547 and E501-H523 π interactions were disconnected, the π interactions shifted from W521-F524 to W521-V525 and from W493-Y451 to F489-F451. Even if the D512-S515 and Q514-S518 H-bonds were also broken, F526 still had a π–π interaction with Y565. In the VSLD/S4-S5linker/TRP interfaces, the T566-S576 H-bond and the Q570-W692 and Y575-I579 π interactions were disrupted with the shift of the H-bond from Q570-R690 to Q570-R693 and the reemployment of the E687-R690 salt bridge. In the TRP/pre-S1/VSLD interfaces, the T397-K432/E704 and T411-D519 and H417/E418-R690 H-bonds and the K432-E704 salt bridge and the F441-W433 π interaction were replaced with the Y409-K705/R698 H-bonds as well as the reinstatement of the R698-E702 salt bridge.

When these conformational changes expanded to the pore domain, the broken non-covalent interactions included the E610-T649 and K614-S620/N647 and E631-K634 H-bonds, and the F597-F601 and Y622-F654 and F633-I637 π interactions. When the H-bond moved from S624-D627 to Y622-S626 pairs and the π interaction shifted from Q646-F654 to N647-F654 pairs, E679 also formed an H-bond with N683.

As a result, the fourth biggest little hairpin with one equivalent H-bond in a minimum 13-residue loop appeared in the pre-S1/TRP interface (Fig.4B). It controlled the D396-K432 salt bridge via the Y409-R698 H-bond and the R696-W433 π interaction (Fig. 4C-D). In this case, the removal of the PC lipid from the vanilloid site decreased the temperature threshold from 50°C to 38°C as calculated (Table 1). This melting temperature was near the experimental threshold 37°C [19]. In the meanwhile, the total numbers of all non-covalent interactions and minimum little

hairpin sizes along the gating pathway from D396 to K705 also reduced from 69 and 101 to 44 and 92, respectively (Fig. 4A).

2.6. Release of the PC Lipid from the Vanilloid Site by the Y564A Mutation Decreased the Temperature Sensitivity of Reduced mTRPV3

When the mTRPV3-Y564A mutant opened with the fourth biggest little hairpin in the TRP/pre-S1 interface melting at 37°C, the disruption of the D396-K432 salt bridge triggered several changes. In the VSLD/pre-S1/TRP interfaces, the Y409-K705/R698 H-bonds and the R416-D519 salt bridge were substituted by the Y409-L508 π interaction and the T411-S515 H-bond, respectively (Figs. 5A-B, E). When H417 formed an H-bond with E689, the E702-K500 H-bond and the R698-D519 salt bridge also replaced the R698-E702 salt bridge. In the S4-S5 linker/TRP interface, the Q570-R693 H-bond moved to the Q570-W692 π interaction with the broken E689-R693 H-bond (Fig. 5A).

When these conformational changes extended to the pore domain, the D586-R579 H-bond and the F597-F601 π interaction and the E631-K634 salt bridge were restored with the broken Y622-S626 and E679-N683 H-bonds. In addition, the π interaction moved from N647-F654 to S648-F654 (Fig. 5A).

When the conformational wave expanded to the VSLD, the π–π interaction shifted from F445-Y565 to F445-F441 pairs. When the F450-F489 π interaction and the Y448-Q529 H-bond were disrupted, both the R464-D468 salt bridge and the H477-W481 π interaction were present. On the other hand, when the W521-F522 and F524-V528 π interactions were disconnected, the F522-F526 and Y540-Y547 and F542-Y544 π interactions were present again (Fig. 5A).

By all accounts, the fifth biggest little hairpin appeared in the TRP/VSLD/pre-S1 interfaces. It had a minimum 14-residue loop from Y448 to F447, W493, K500, E702, Q695, R567, Y565 and back to Y448 (Fig. 5A, C-E). The presence of three equivalent H-bonds in the loop set the melting temperature as 56°C (Table 1). Therefore, this Y564A mutant may have an upper temperature limit 56°C. In any way, the total numbers of all non-covalent interactions and minimum little hairpin sizes along the gating pathway from D396 to K705 had small changes from 44 and 92 to 45 and 90, respectively (Fig. 5A). Therefore, the calculated structural thermo-sensitivity Ω_{10} was in a range from 0.51 to 2.93 and with a mean value 1.00, which was comparable to the experimental functional thermo-sensitivity Q_{10} (~1.21). [19] In other words, the removal of

the PC lipid from the vanilloid site dramatically weakened the structural and functional thermo-sensitivity.

3. DISCUSSION

Although protein and DNA use sequences of amino acids and nucleotides to form primary polypeptide and polynucleotide chains, respectively, an alteration in the loop sequence has no significant effect on the melting temperature of the DNA hairpin. [17] Therefore, when an intramolecular non-covalent interaction creates a topological hairpin, the hairpin should be thermodynamically and chemically equivalent between DNA and protein.

At a given salt concentration (150 mM NaCl), a DNA hairpin with a 20-base long poly-A loop has a temperature threshold 34°C. When the loop size decreases from 20 to 10 bases or the H-bonded base pairs in the stem increase from 2 to 4, the threshold can be increased more than 20 degrees. [17] If the biggest little hairpin undergoes a single-step melting reaction similarly to DNA hairpins to initiate a temperature threshold for mTRPV3 activation, the calculated melting temperature (T_m) should be comparable to the experimental threshold (T_{th}) for channel activation. For reduced mTRPV3, the calculated T_m of the third biggest little hairpin with a minimum 12-carbon loop and 2.0 equivalent H-bonds was 50°C. This value was similar to the initial T_{th} 50°C for reduced mTRPV3 activation. [26] For oxidized mTRPV3, the calculated T_m of the first biggest little hairpin with a minimum 17-residue loop and 2.0 equivalent H-bonds was about 40°C, which was close to the experimental T_{th} 42°C. [18] For reduced mTRPV3-Y564A, the fourth biggest little hairpin with a minimum 13-residue loop and 1.0 equivalent H-bonds resulted in a calculated T_m 38°C, which was near the experimental threshold 37°C (Table 1). [19]

In addition the similarity between T_m and T_{th}, the calculated structural thermo-sensitivity Ω_{10} was also comparable to the functional thermo-sensitivity Q_{10}. For example, reduced mTRPV3 had an experimental Q_{10} value 21.2 while the calculated mean Ω_{10} was about 22.8. [26] When this channel was oxidized, the Q_{10} and Ω_{10} values were 27.0 and 21.0, respectively. [18] For reduced mTRPV3-Y564A, the Q_{10} and Ω_{10} values were 1.21 and 1.00, respectively. [19] In this regard, when the intensity of a non-covalent interaction was in the range from 0.5 to 3 kJ/mol, the Q_{10} ranges from the minimal to the maximal may be theoretically calculated as 10.2-82.6 for reduced mTRPV3, 9.34-76.0 for oxidized mTRPV3, and 0.51-2.93 for reduced mTRPV3-Y5674A (Table 1).

Taken together, when reduced mTRPV3 is activated above 50°C upon the melting of the third biggest little hairpin, C612 may be close to C619 enough to produce a disulfide bond (Figs. 2-3). When oxidized mTRPV3 is closed below 50°C, the first biggest little hairpin decreased the activation threshold to 40°C (Fig. 1-2). [18] This lower threshold may increase the open probability so that mTRPV3 activation exhibits use-dependent sensitization upon successive heat stimuli [7, 18-21, 23]. On the other hand, because the removal of the PC lipid from the vanilloid site could decrease the threshold to 38°C but the calculated T_m of the second and fifth biggest little hairpins in the open states was about 56°C (Figs. 2, 5), the measurable range of thermo-gated mTRPV3 may be at least from 38°C to 56°C (Table 1). Therefore, the biggest little hairpins along the gating pathway may be responsible for the temperature thresholds and the measureable limit of the mTRPV3 bio-thermometer in a redox- and PC lipid-dependent manner.

Since a smaller hairpin has a higher melting temperature and thus a larger heat capacity [17], the higher Q_{10} in mTRPV3 may result from the dramatic decrease in the total minimum loop sizes in little hairpins along the gating pathway upon a concurrent change in the total non-covalent interactions. When a PC lipid binds at the vanilloid site to increase the initial total little hairpin sizes, it may also enhance the temperature sensitivity of mTRPV3. [18] Thus, it is reasonable that the release of that PC lipid may result in a low Q_{10} in response to the second heat stimulus (Table 1). [26]

In addition to the biggest little hairpins for the thresholds, smaller little hairpins may be required for heat-evoked mTRPV3 opening. Some were state- and redox-independent no matter whether the stimulus is physical or chemical (Figs. 1-3). Therefore, they may form a basic stable backbone anchor system for mTRPV3 activation or a heat fuse group to prevent heat denaturation or channel deactivation [18-20].

The first had no residue in the loop from Y594 to T636 and Y661 and back to Y594. The mutation N643S, I644S, N647Y, L657I, or Y661C in the outer pore is factually less sensitive to heat [27], possibly because those mutations may destablize that smallest little hairpin and thus decrease the heat efficacy (Figs. 1-3). In addition, the T636S mutation also decreases the temperature threshold [28], possibly owing to the mutation-induced formation of a new biggest little hairpin with a size larger than 12-carbon in the minimum loop or the weakened non-covalent interactions in the biggest little hairpin loop along the gating pathway (Fig.3).

The second had a minimum 9-residue loop from D586 to F590, L673 and T680 and then back to D586 (Fig. 2A). In agreement with this importance, the T680A mutation suppresses the heat-evoked opening of reduced mTRPV3 with the N-terminal 1–117 residues truncated [25].

The third had a minimum 4-residue loop from T411 to R416 and D519 and then back to T411 (Fig. 3A). When the insertion of valine or serine at position 412 disrupts the T411-D519 H-bond, another biggest little hairpin with a larger minimum loop may be formed in the VSLD/pre-S1/TRP interfaces and thus dramatically decrease the threshold and sensitivity like reduced mTRPV3-Y564A (Fig.5, Table 1). [19, 26]

The fourth had no residue in the loop from Y448 to F526, Y564, Y565 and back to Y448 (Figs. 1-3). It has been reported that the Y564A mutation decreases the threshold of reduced mTRPV3 from 50°C to 37°C and the temperature sensitivity Q_{10} from 21.2 or 27 to 1.2 [19, 26].

Finally, further experiments may be necessary to test if non-covalent interactions in other smaller little hairpins are essential for heat-evoked TRPV3 opening. For example, the D519-R416/R567 salt or H-bonding bridges, the T566-S576 and R567-Q695 and S622-Q646 and T636-Y594-Y661-T636 H-bonds, the Y622-F654 and F441/F445/Y448-Y565 and Y448-F526/Y565 π–π interactions, and the W692-R696-W433-K438 cation-π interactions (Fig. 2A).

4. METHODS

4.1 Data Mining Resources

In this computational study, the cryo-EM structural data of oxidized mTRPV3 with a high resolution in different gating and redox states at 42°C were first analyzed with graph theory, a novel tool, to reveal the roles of the little hairpins with minimum loop sizes and strengths in regulating the temperature threold and the thermosensitivity of TRPV3. They include closed and reduced mTRPV3 in MSP2N2 (PDB ID, 6LGP, model resolution= 3.31 Å), [25] closed and oxidized mTRPV3 in cNW11 (PDB ID, 7MIN, model resolution= 3.09 Å), and open and oxidized mTRPV3 in cNW11 (PDB ID, 7MIO, model resolution= 3.48 Å) [18]. In addition, the cryo-EM structural data of detergent-solubilized and reduced mTRPV3-Y564A in the sensitized but closed state (PDB ID, 6PVO, model resolution= 5.18 Å) and in the open state at 37°C (PDB ID, 6PVP, model resolution= 4.4 Å) were also analyzed as controls to uncover the role of the PC lipid in increasing the temperature threshold and sensitivity of TRPV3 [19].

4.2 Standards for Non-covalent Interactions

Structure visualization software, UCSF Chimera, was used to assess the presence of non-covalent interactions in TRPV3. Since the gating of thermosensitive TRP channels is governed by stereo- or regioselective inter- or intradomain interactions, only stereo- or regioselective diagonal and lateral non-covalent interactions were included in this study to test their potential roles in forming minimum little hairpin topological loops to control the temperature threshold and sensitivity. They included salt-bridges, CH/cation/lone pair/π–π interactions and H-bonds along the gating pathway in mTRPV3 with or without the Y564A mutation. In contrast, the hydrophobic interactions were not considered because they lack both stereo- and regio-selectivity [29].

The standard definition of noncovalent interactions was employed. A hydrogen bond was considered present when the angle donor-hydrogen-acceptor was within the cut-off of 60°, and when the hydrogen-acceptor distance is within 2.5 Å and the maximum distance is 3.9 Å between a donor and an acceptor. A salt bridge was considered to be formed if the distance between any of the oxygen atoms of acidic residues and the nitrogen atoms of basic residues were within the cut-off distance of 3.2-4 Å in at least one frame. When the geometry was acceptable, a salt bridge was also counted as a hydrogen bonding pair. The face-to-face π-π stacking of two aromatic rings was considered effective once the separation between the π-π planes was ~3.35-4.4 Å, which is close to at least twice the estimated van der Waals radius of carbon (1.7Å). The edge-to-face π-π interaction of two aromatic rings was considered attractive when the cut-off distance between two aromatic centers was within 4-6.5 Å. Significant cation- π interactions occured within a distance of 6.0 Å between a cation and an aromatic center. The short effective CH/π distances was 2.65-3.01 Å between aromatic groups, and 2.75-2.89 Å between CH_3 and an aromatic ring. The lone pair-π interaction distance between a lone electron pair and an aromatic ring was within 3-3.7 Å.

4.3 Preparation of Little Hairpin Topological Loop Maps by Using Graph Theory

After non-covalent interactions were scanned along the gating pathway of mTRPV3 from D396 in the pre-S1 domain to K705 in the TRP domain, graph theory was used as a novel tool to define the minimum loop size in little hairpins to control every non-covalent interaction and geometrically to realize the little hairpin topological loop maps along the gating pathway in the closed, sensitized or open states at 4°C, 37°C and 42°C. The primary amino acid sequence line from D396 to K705 was marked in black. An amino acid side chain involving a non-covalent interaction along the gating pathway of mTRPV3 was defined as a vertex and marked with an arrow in different colors. The same kind of non-covalent interactions between two amino acid

side chains was marked with an edge in the same color. A little hairpin topologicval loop was considered significant when an edge forms a sealed topological ring with the amino acid sequence between two ends of the edge or other edges. The minimum loop size L was definded as the number of residues that did not participate in any non-covalent interctions in the little hairpin loop with a minimum size which was marked in black. The biggest and smaller little hairpin sizes for channel gating were shown in red circles. The total number of all noncovalent interactions and minimum little hairpin loop sizes along the gating pathway were shown in black and blue circles, respectively.

4.4 Calculation of the Temperature Threshold of mTRPV3

The temperature threshold was calculated from the melting temperature T_m of the biggest little hairpin along the gating pathway using the following equation: [17]

$$T_m\ (°C) = 34 + (n-2)\times 10 + (20-L_{max})\times 2$$

where, n is the total number of the non-covalent interactions equivalent to H-bonds in the biggest little hairpin, and L_{max} is the loop length of the biggest little hairpin.

4.5 Calculation of the Temperature Sensitivity of mTRPV3

If a thermosensitive ion channel changes from a closed state to an open state within a temperature range ΔT, $\Omega_{\Delta T}$ was used to evaluate the structural thermo-sensitivity of a single ion channel as calculated using the following equation:

$$\Omega_{\Delta T} = [(L_o-L_c)E/2]^{(Nc/No)}$$

where, L_o and L_c are the total numbers of all the minimum lengths of little hairpins along the gating pathway in the open and closed states, respectively; N_c and N_o are the total numbers of all the non-covalent interactions along the gating pathway in the closed and open states, respectively; E is the energy intensity of a non-covalent interaction in a range of 0.5-3 kJ/mol. Usually, E=1 kJ/mol.

When ΔT=10°C, Ω_{10} could be comparable to the functional thermo-sensitivity Q_{10} of a single ion channel. Q_{10} was calculated using the following equation:

$$Q_{10} = (R2/R1)^{10/(T2-T1)}$$

where, R1 and R2 are rates of a reaction at two different temperatures T1 and T2 in Celsius degrees or kelvin, respectively.

Conventions and Abbreviations: ARD, ankyrin repeat domain; cryo-EM, cryo-electron microscopy; T_m, melting temperature; PC, phosphatidylcholine; T_{th}, temperature threshold; TMD,

transmembrane domain; TRP, transient receptor potential; TRPV3, TRP vanilloid-3; mTRPV3, mouse TRPV3; VSLD, voltage-sensor-like domain.

Acknowledgements

The author's own studies cited in this article were supported by NIDDK Grant (DK45880 to D.C.D.) and Cystic Fibrosis Foundation grant (DAWSON0210) and NIDDK grant (2R56DK056796-10) and American Heart Association (AHA) Grant (10SDG4120011 to GW).

Conflict of Interest: The author declares no conflict of interest.

Data Availability Section: This study includes no data deposited in external repositories.

References

1. Caterina, M.J., Schumacher M.A., Tominaga M., Rosen T.A, Levine J.D. and Julius D. The capsaicin receptor: a heat-activated ion channel in the pain pathway. *Nature*. **389(6653),** 816-824. (1997)
2. Caterina, M.J., Rosen T. A., Tominaga M., Brake A. J, Julius D. A capsaicin-receptor homologue with a high threshold for noxious heat. *Nature.* **398,**436. (1999)
3. McKemy D. D., Neuhausser W. M. & Julius D. Identification of a cold receptor reveals a general role for TRP channels in thermosensation. *Nature.* **416(6876),** 52–58. (2002)
4. Peier, A.M., Moqrich A., Hergarden A.C., Reeve A.J., Andersson D.A., Story G.M., Earley T.J., Dragoni I., McIntyre P., Bevan S. and Patapoutian A. A TRP channel that senses cold stimuli and menthol. *Cell*. **108(5),** 705–715. (2002)
5. Peier A. M., Reeve A. J., Andersson D.A., Moqrich A., Earley T.J., Hergarden A.C., Story G.M., Colley S., Hogenesch J. B., McIntyre P., Bevan S., Patapoutian A. A heat-sensitive TRP channel expressed in keratinocytes. *Science*. **296,** 2046. (2002)
6. Smith G. D., Gunthorpe M. J., Kelsell R. E., Hayes P. D., Reilly P., Facer P., Wright J. E., Jerman J. C., Walhin J-P., Ooi L., Egerton J., Charles K. J., Smart D., Randall A. D., Anand P., Davis J. B. TRPV3 is a temperature-sensitive vanilloid receptor-like protein. *Nature.* **418,** 186. (2002)
7. Xu H., Ramsey I. S., Kotecha S. A., Moran M. M., Chong J. A., Lawson D., Ge P., Lilly J., Silos-Santiago I., Xie Y., DiStefano P. S., Curtis R., Clapham D. E. TRPV3 is a calcium-permeable temperature-sensitive cation channel. *Nature.* **418,** 181. (2002)
8. Guler A.D., Lee H., Iida T., Shimizu I., Tominaga M.and Caterina M. J. Heat-evoked activation of the ion channel, TRPV4. *J Neurosci.* **22,** 6408–14. (2002)
9. Chung M. K., Lee H., Caterina M. J. Warm temperatures activate TRPV4 in mouse 308 keratinocytes. *J. Biol. Chem*. **278,** 32037. (2003)
10. Story, G.M., Peier A.M., Reeve A.J., Eid S.R., Mosbacher J., Hricik T.R., Earley T.J., Hergarden A.C., Andersson D.A., Hwang S.W., McIntyre P., Jegla T., Bevan S., Patapoutian A. ANKTM1, a TRP-like channel expressed in nociceptive neurons, is activated by cold temperatures. *Cell*. **112,** 819–829. (2003)

11. Jordt, S.E., Bautista D.M., Chuang H.H., McKemy D.D., Zygmunt P.M., Högestätt E.D., Meng I.D. and Julius D. Mustard oils and cannabinoids excite sensory nerve fibres through the TRP channel ANKTM1.*Nature.* **427,** 260–265. (2004)
12. Talavera K, Yasumatsu K., Voets T., Droogmans G., Shigemura N., Ninomiya Y., Margolskee R. F., Nilius B. Heat activation of TRPM5 underlies thermal sensitivity of sweet taste. *Nature.* **438,** 1022. (2005**)**
13. Vriens J, Owsianik G., Hofmann T., Philipp S., Stab J., Chen X., Benoit M., Xue F., Janssens A., Kerselaers S., Oberwinkler J., Vennekens R., Gudermann T., Nilius B., Voets T. TRPM3 is a nociceptor channel involved in the detection of noxious heat. *Neuron.* **70,** 482. (2011)
14. Zimmermann,K., Lennerz J.K., Hein A., Link A.S., Kaczmarek J.S., Delling M., Uysal S., Pfeifer J.D., Riccio A. and Clapham D.E. Transient receptor potential cation channel, subfamily C, member 5 (TRPC5) is a cold-transducer in the peripheral nervous system. *Proc. Natl. Acad. Sci.USA*. **108,** 18114–18119. (2011)
15. Song K., Wang H., Kamm G. B., Pohle J., Reis F. C., Heppenstall P., Wende H., Siemens J. The TRPM2 channel is a hypothalamic heat sensor that limits fever and can drive hypothermia. *Science.* **353,**1393. (2016)
16. Tan C. H., McNaughton P. A. The TRPM2 ion channel is required for sensitivity to warmth. *Nature.* **536,** 460. (2016)
17. Jonstrup A.T., Fredsøe J., Andersen A.H. DNA Hairpins as Temperature Switches, Thermometers and Ionic Detectors. *Sensors.* **13,** 5937-5944. (2013**)**
18. Nadezhdin, K. D., Neuberger, A., Trofimov, Y. A., Krylov, N. A., Sinica, V., Kupko, N., Vlachova, V., Zakharian, E., Efremov, R. G., and Sobo-levsky, A. I. Structural mechanism of heat-induced opening of a temperature-sensitive TRP channel. *Nat. Struct. Mol. Biol.* **28,** 564–572. (2021)
19. Singh, A.K., McGoldrick L.L., Demirkhanyan L., Leslie M., Zakharian E., and Sobolevsky A.I. Structural basis of temperature sensation by the TRP channel TRPV3. *Nat. Struct. Mol. Biol.* **26,** 994–998. (2019)
20. Singh, A.K., McGoldrick L.L. and Sobolevsky A.I. Structure and gating mechanism of the transient receptor potential channel TRPV3. *Nat. Struct. Mol. Biol.* **25,** 805–813. (2018)

21. Zubcevic, L., Herzik Jr. M. A., Wu M., Borschel W.F., Hirschi M., Song A.S., Lander G.C., and Lee S. Y. Conformational ensemble of the human TRPV3 ion channel. *Nat. Commun.* **9,** 4773. (2018**)**
22. Liao M, Cao E., Julius D. & Cheng Y. Structure of the TRPV1 ion channel determined by electron cryo-microscopy. *Nature.* **504,**107. (2013**)**
23. Liu B.Y., Yao J., Zhu M.X. & Qin F. Hysteresis of gating underlines sensitization of TRPV3 channels. *J. Gen. Physiol.* **138,** 509–520. (2011)
24. Liu B. & Qin F. Use dependence of heat sensitivity of vanilloid receptor TRPV2. *Biophys J.* **110(7),** 1523–1537. (2016)
25. Shimada, H., Kusakizako, T., Nguyen, THD, Nishizawa, T., Hino T., Tominaga M., Nureki, O. The structure of lipid nanodisc-reconstituted TRPV3 reveals the gating mechanism. *Nat Struct Mol Biol.* **27,** 645-652. (2020)
26. Liu, B. & Qin F. Single-residue molecular switch for high-temperature dependence of vanilloid receptor TRPV3. *Proc. Natl.Acad. Sci. USA.* **114,** 1589–1594. (2017)
27. Grandl JH, Hu H, Bandell M, Bursulaya B, Schmidt M, Petrus M and Patapoutian A. Pore region of TRPV3 ion channel is specifically required for heat activation. *Nat. Neurosci*. **11,** 1007–1013. (2008)
28. Myers B. R., Bohlen C. J., Julius D. A yeast genetic screen reveals a critical role for the pore helix domain in TRP channel gating. *Neuron.* **58,** 362-273. (2008)
29. Baumgartner A. Insertion and Hairpin Formation of Membrane Proteins: A Monte Carlo Study. *Biophys. J.* **71,** 1248-1255. (1996**)**

Figure legends

Figure 1. **The little hairpin topological structural network along the gating pathway of PC-bound oxidized mTRPV3 in the closed state at 42°C. A,** The little hairpin topological loop map. The cryo-EM structure of closed and oxidized mTRPV3 with PC bound in cNW11 at 42°C (PDB ID, 7MIN) was used for the model.[18] The pore domain, the S4-S5 linker, the TRP domain, the VSLD and the pre-S1 domain are indicated in black. Salt bridges, π interactions, and H-bonds between pairing amino acid side chains along the gating pathway from D396 to K705 are marked in purple, green, and orange, respectively. The minimum loop sizes in the little hairpins required to control the relevant non-covalent interactions are labeled in black. The total numbers of all minimum little hairpin loop sizes and non-covalent interactions along the gating pathway are shown in the blue and black circles, respectively. **B,** The PC lipid at the vanilloid site. **C,** The location of the 1st biggest little hairpin. **D,** The structure of the 1st biggest little hairpin with a minimum 17-residue loop in the VSLD/pre S1 interface to control the R416-D519 salt bridge. **E,** The sequence of the 1st biggest little hairpin with a minimum 17-residue loop. The R416-D519 salt bridge is marked in a blue box.

Figure 2. **The little hairpin topological structural network along the gating pathway of PC-free oxidized mTRPV3 in the open state at 42°C. A,** The little hairpin topological loop map. The cryo-EM structure of open mTRPV3 without PC bound in cNW11 at 42°C (PDB ID, 7MIO) was used for the model.[18] The pore domain, the S4-S5 linker, the TRP domain, the VSLD and the pre-S1 domain are indicated in black. Salt bridges, π interactions, and H-bonds between pairing amino acid side chains along the gating pathway from D396 to K705 are marked in purple, green, and orange, respectively. The minimum loop sizes in the little hairpins required to control the relevant non-covalent interactions are labeled in black. The total numbers of all minimum little hairpin loop sizes and non-covalent interactions along the gating pathway are shown in the blue and black circles, respectively. **B,** The location of the 2nd biggest little hairpin **C,** The structure of the 2nd biggest little hairpin with a minimum 9-residue loop in the S5-S6 interface to control the stimulatory D586-T680 H-bond. **D,** The structure of the little hairpin for the lower gate. **E,** The sequences of two little gating hairpins with minimum 9- and 3-residue loops to control the D586-T680 H-bond and three crtitical non-covalent interactions in the blue boxes, respectively.

Figure 3. **The little hairpin topological structural network along the gating pathway of PC-bound reduced mTRPV3 in the closed state at 4°C. A,** The little hairpin topological loop map. The cryo-EM structure of reduced and closed mTRPV3 with PC bound in MSP2N at 4°C (PDB ID, 6LGP) was used for the model.[25] The pore domain, the S4-S5 linker, the TRP domain, the VSLD and the pre-S1 domain are indicated in black. Salt bridges, π interactions, and H-bonds between pairing amino acid side chains along the gating pathway from D396 to K705 are marked in purple, green, and orange, respectively. The minimum loop sizes in the little hairpins required to control the relevant non-covalent interactions are labeled in black. The total numbers of all minimum little hairpin loop sizes and non-covalent interactions along the gating pathway are shown in the blue and black circles, respectively. **B,** The location of the 3rd biggest little hairpin. **C,** The structure of the 3rd biggest little hairpin with a minimum 12-carbon loop in the VSLD to control the W521-PC-F524 bridge. **D,** The sequences of the 3rd biggest little hairpin with a minimum 12-carbon loop to control the W521-PC-F524 bridge in the blue rectangle.

Figure 4. **The little hairpin topological structural network along the gating pathway of PC-free reduced mTRPV3-Y564A in the sensitized but closed state at 37°C. A,** The little hairpin topological loop map. The cryo-EM structure of detergent-solubilzed and sensitized and reduced mTRPV3 without PC bound at 37°C (PDB ID, 6PVO) was used for the model.[19] The pore domain, the S4-S5 linker, the TRP domain, the VSLD and the pre-S1 domain are indicated in black. Salt bridges, π interactions, and H-bonds between pairing amino acid side chains along the gating pathway from D396 to K705 are marked in purple, green, and orange, respectively. The minimum loop sizes in the little hairpins required to control the relevant non-covalent interactions are labeled in black. The total numbers of all minimum little hairpin loop sizes and non-covalent interactions along the gating pathway are shown in the blue and black circles, respectively. **B,** The location of the 4th biggest little hairpin. **C,** The structure of the 4th biggest little hairpin with a minimum 13-residue loop in the TRP/pre S1 interface to control the D396-K432 salt bridge. **D,** The sequences of the 4th biggest little hairpin with a minimum 13-residue loop to control the D396-K432 salt bridge in the blue rectangle.

Figure 5. **The little hairpin topological structural network along the gating pathway of PC-free reduced mTRPV3-Y564A in the open state at 37°C. A,** The little hairpin topological loop map. The cryo-EM structure of detergent-solubilzed and open mTRPV3-Y564A without PC bound in cNW11 at 37°C (PDB ID, 6PVP) was used for the model.[19] The pore domain, the S4-S5 linker, the TRP domain, the VSLD and the pre-S1 domain are indicated in black. Salt bridges, π interactions, and H-bonds between pairing amino acid side chains along the gating pathway from D396 to K705 are marked in purple, green, and orange, respectively. The minimum loop sizes in the little hairpins required to control the relevant non-covalent interactions are labeled in black. The total numbers of all minimum little hairpin loop sizes and non-covalent interactions along the gating pathway are shown in the blue and black circles, respectively. **B,** The strucutre of a little hairpin with a minimum 3-residue loop for the T411-S515 H-bond. **C,** The location of the 5th biggest little hairpin. **D,** The structure of the 5th biggest little hairpin with a minimum 14-residue loop in the VSLD/TRP interface to control the stimulatory K500-E702 H-bond. **E,** The sequences of two little gating hairpins with minimum 3- and 14-residue loops to control the T411-S515 H-bond/the L508-Y409 π interaction and the K500-E702 H-bond/the F447-W493 π interaction in the blue boxes, respectively.

Figures

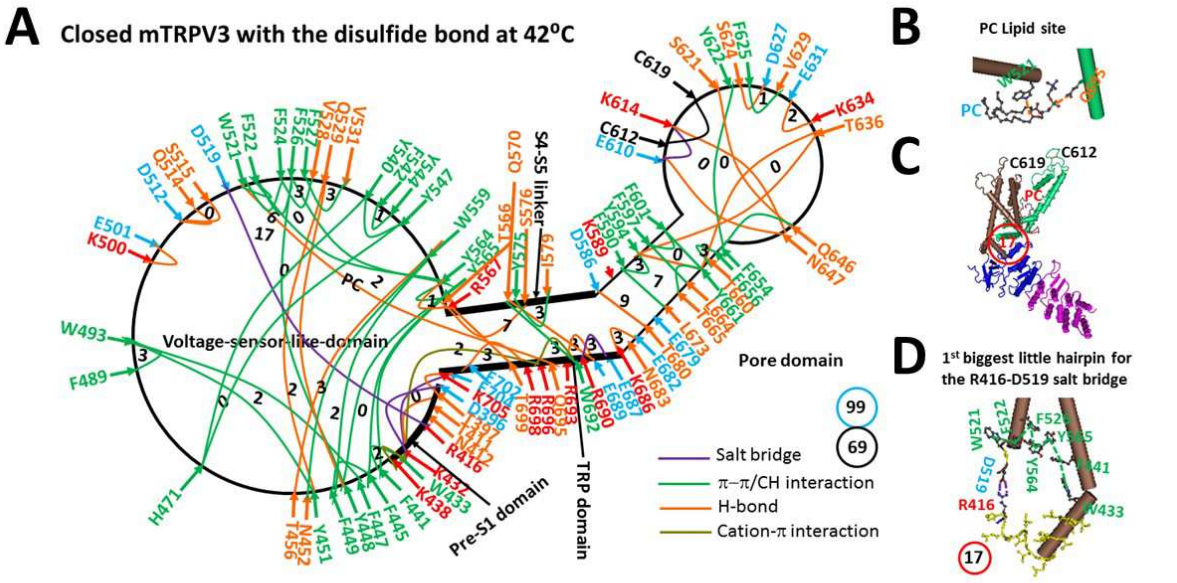

Figure 1

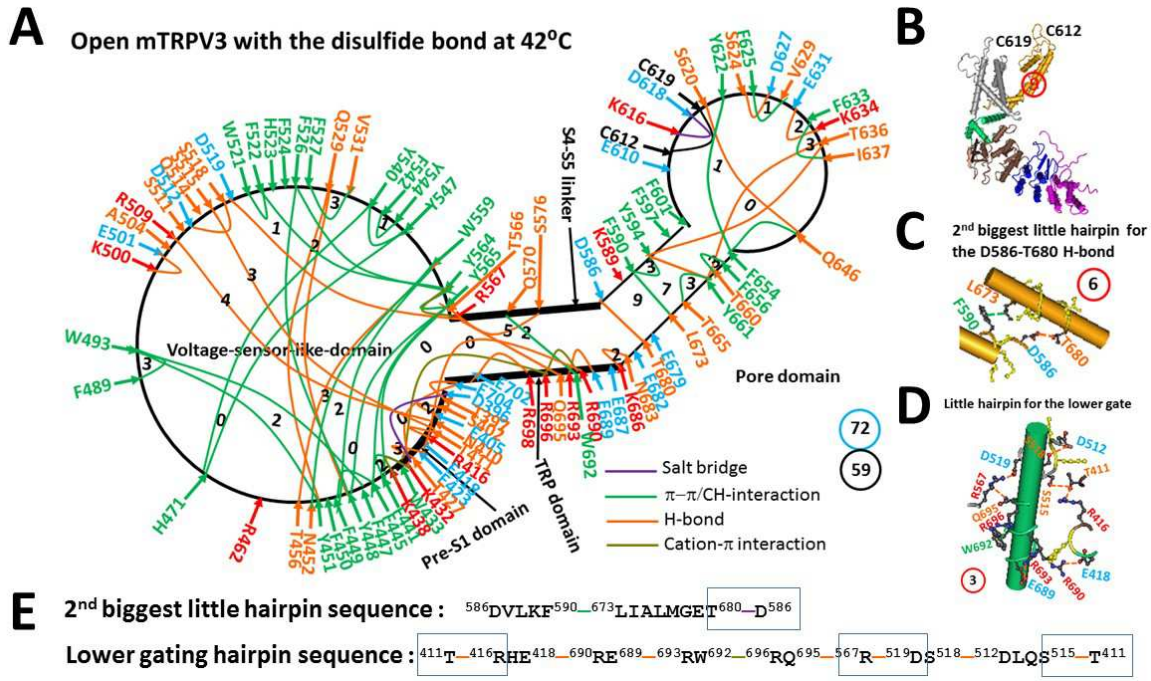

Figure 2

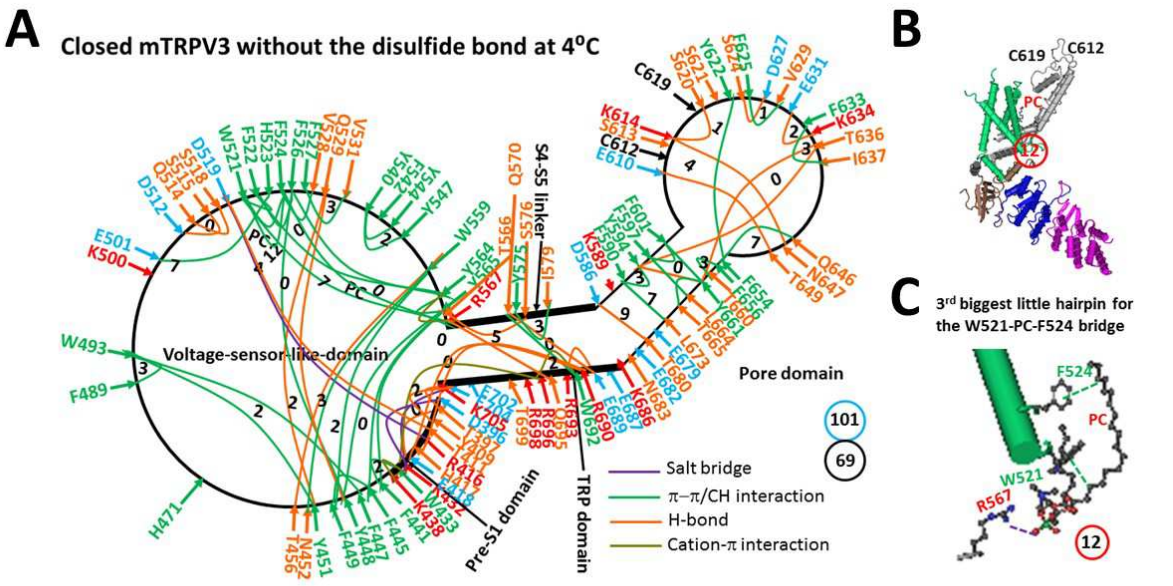

D 3rd biggest little hairpin sequence : ^{521}W–PC–F^{524}–W^{521}

Figure 3

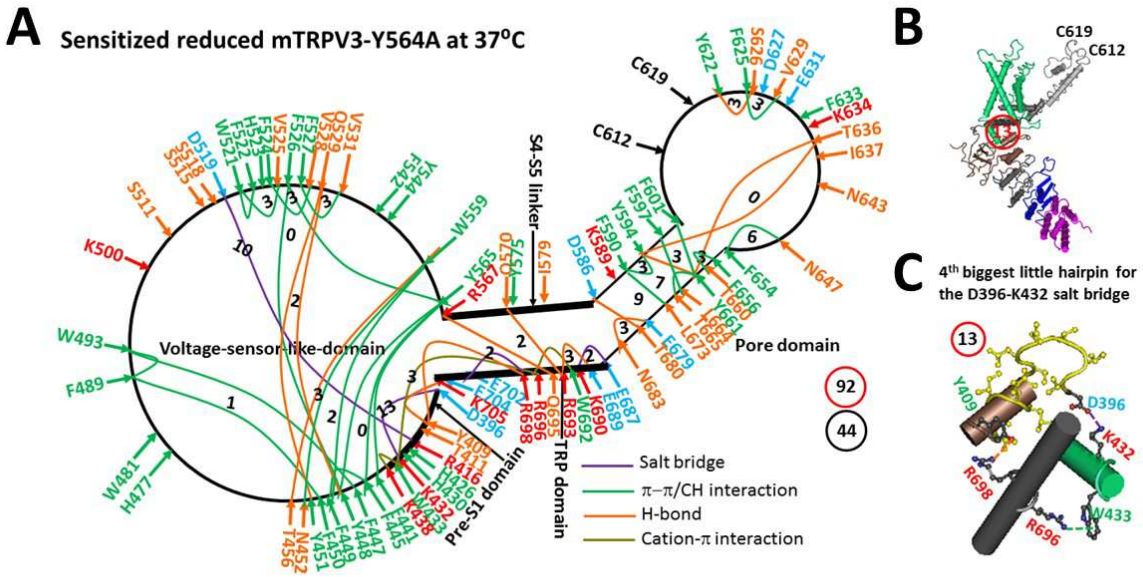

D 4th biggest little hairpin sequence : ^{396}DTTTDNSVLEIIVY^{409}–^{698}RAR^{696}–^{433}WK^{432}–^{396}D

Figure 4

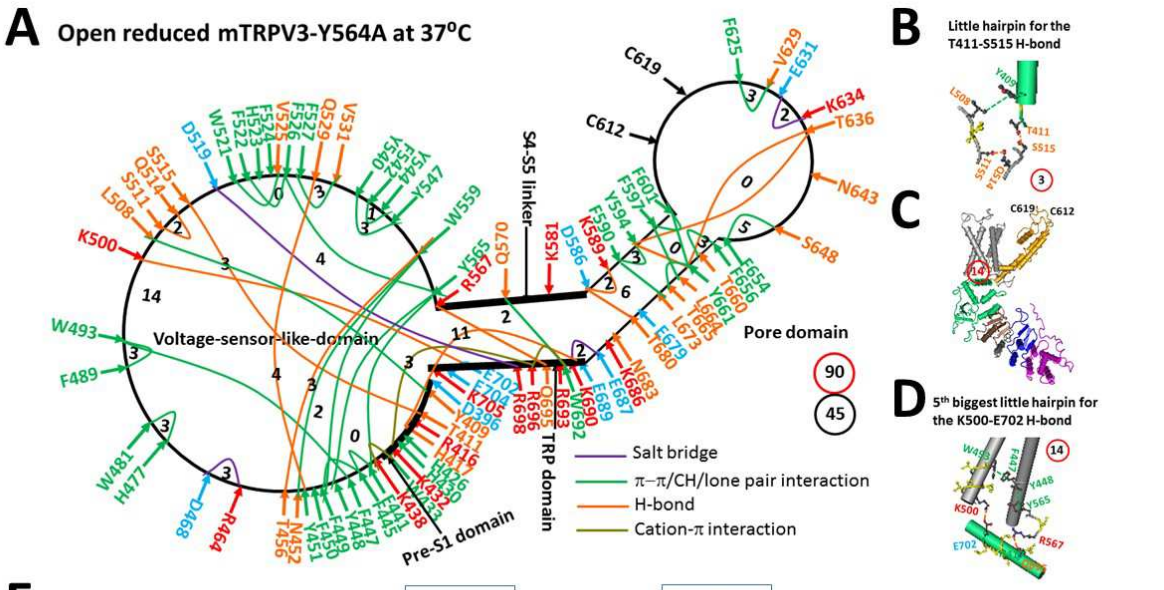

E **Little hairpin sequence :** ^{409}YNT^{411}–^{515}SQ^{514}–^{511}SPRL^{508}–^{409}Y

5th biggest little hairpin sequence : ^{448}YF^{447}–^{493}WATCISVK^{500}–^{702}ELITRARQ^{695}–^{567}RTY^{565}–^{448}Y

Figure 5